Effects of Fullerene Bisadduct Regioisomers on Photovoltaic Performance

Xiangyue Meng, Guangyao Zhao, Qi Xu, Zhan'ao Tan, Zhuxia Zhang, Li Jiang, Chunying Shu, Chunru Wang, and Yongfang Li**

Fullerene bisadducts have emerged as promising electron-accepting materials because of their ability to increase the open-circuit voltage (V_{OC}) of polymer solar cells (PSCs) due to their relatively high lowest unoccupied molecular orbital (LUMO) energy levels. It should be noted that the as-prepared fullerene bisadducts are in fact a mixture of isomers. Here, the effects of fullerene bisadduct regioisomers on photovoltaic performance are examined. The *trans*-2, *trans*-3, *trans*-4, and e isomers of dihydronaphthyl-based [60] fullerene bisadduct (NCBA) are isolated and used as acceptors for P3HT-based PSCs. The four NCBA isomers exhibit different absorption spectra, electrochemical properties, and electron mobilities, leading to varying PCE values of 5.8, 6.3, 5.6, and 5.5%, respectively, which are higher than that based on an NCBA mixture (5.3%), suggesting the necessity to use the individual fullerene bisadduct isomer for high-performance PSCs.

1. Introduction

Polymer solar cells (PSCs) offer great potential as a low cost solar energy conversion technology due to their ability to be solution processed over large areas.[1] The last decade has yielded a tremendous improvement in the power conversion efficiency (PCE) of bulk heterojunction (BHJ) PSCs.[2] Impressive PCEs of 9.2% and 10.6% have been reported in the literatures for a single layer BHJ PSC and a multi-layer tandem PSC, respectively.[3,4] The dramatic improvement of PSC performance is ascribed to the design of new semiconducting materials (donor[5] and acceptor[6]) and to the growing understanding of PSC device operation.

It is well-established that the open-circuit voltage (V_{oc}) is proportional to the difference between the lowest unoccupied molecular orbital (LUMO) energy level of the acceptor and the highest occupied molecular orbital (HOMO) energy level of the donor.[7] Hence, Raising the LUMO of the acceptor is preferred for increasing the V_{oc} values.[8] It has been reported that fullerene bisadduct acceptors effectively enhance the V_{oc} as well as the PCE of P3HT based PSCs because of their higher LUMO energy levels.[9] Successful examples such as [6,6]-phenyl-C_{61}-butyric acid methyl ester bisadduct (bis-PCBM),[10] indene-C_{60} bisadduct (ICBA),[11] di(4-methylphenyl)-methano-C_{60} bisadduct (DMPCBA),[12] and thieno-*o*-quinodimethane-C_{60} bisadduct (TOQC)[13] have been reported for the PCE values of ca. 5%.

Recently, we synthesized a dihydronaphthyl-based [60] fullerene bisadduct derivative (NCBA)[14] with LUMO energy level ca. 0.16 eV higher than that of [6,6]-phenyl-C_{61}-butyric acid methyl ester (PCBM). The V_{oc} and PCE values of the PSC based on P3HT:NCBA reached 0.82 V and 5.37%, respectively. Here, it should be noted that the as-prepared fullerene bisadduct derivative was in fact a mixture of isomers, which were directly used to fabricate PSCs without further separating each isomer. For NCBA, there are eight possible regioisomers (*cis*-1, *cis*-2, *cis*-3, *e*, *trans*-1, *trans*-2, *trans*-3, and *trans*-4, following Hirsch nomenclature,[15]) as shown in **Figure 1**. The current synthetic routes[16] to fullerene bisadducts invariably generate a mixture of isomers which introduces disorder in the molecular packing.[17] which could adversely affect electron transporting properties. The individual fullerene bisadduct isomer with the two substituents at specific positions on fullerene cage might be favorable to reach regular molecular packing, leading to higher electron mobility and higher fill factor of the PSC device. And it has been calculated that different isomers of fullerene bisadducts have different electronic energy levels,[18] which might lead to improved V_{oc} of the PSC device. Therefore, a better photovoltaic performance of the individual fullerene bisadduct isomer is expected, compared

X. Y. Meng, Z. X. Zhang, L. Jiang, Prof. C. Y. Shu, Prof. C. R. Wang
Key Laboratory of Molecular Nanostructure and Nanotechnology
Beijing National Laboratory for Molecular Sciences
Institute of Chemistry
Chinese Academy of Sciences
Beijing, 100190, China
E-mail: crwang@iccas.ac.cn
G. Y. Zhao, Prof. Y. F. Li
Key Laboratory of Organic Solids
Institute of Chemistry
Chinese Academy of Sciences
Beijing, 100190, China
E-mail: liyf@iccas.ac.cn
Q. Xu, Prof. Z. A. Tan
State Key Laboratory of Alternate Electrical Power System with Renewable Energy Sources
The New and Renewable Energy of Beijing Key Laboratory
North China Electric Power University
Beijing, 102206, China
X. Y. Meng, G. Y. Zhao
University of Chinese Academy of Sciences
Beijing, 100049, China.

DOI: 10.1002/adfm.201301411

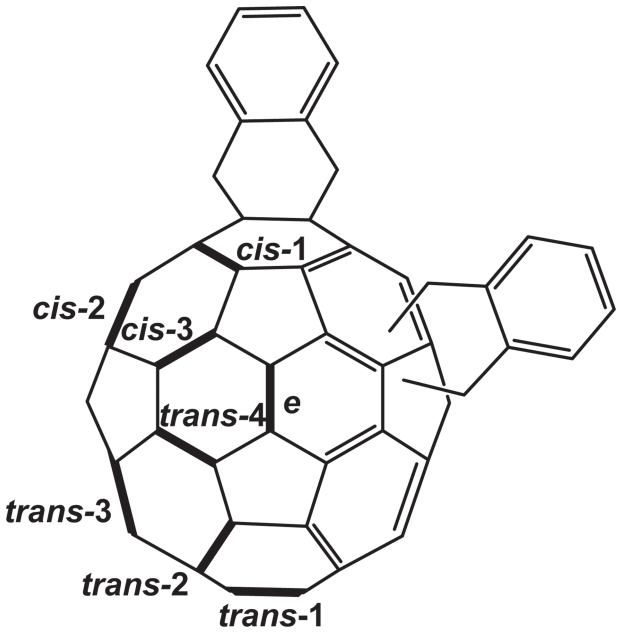

Figure 1. Molecular structure of the eight possible regioisomers for NCBA.

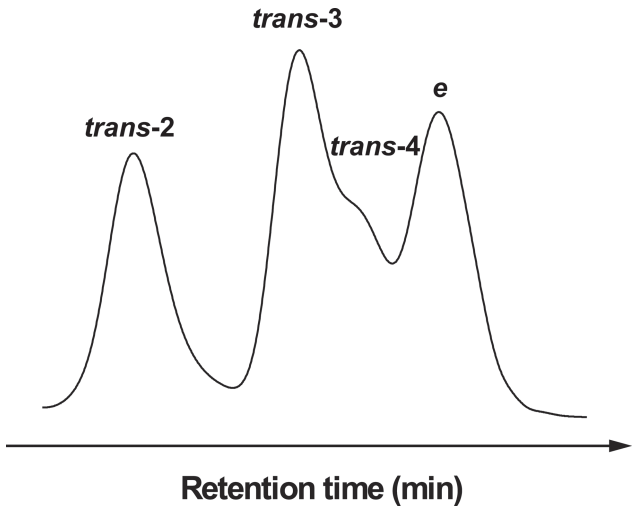

Figure 2. HPLC profile of the NCBA mixture.

to fullerene bisadduct mixture. Moreover, the large-scale production of mixtures of isomers of fullerene bisadducts is likely to suffer from problems in batch-to-batch reproducibility, since different isomer ratio and distribution can occur in the chemical synthesis. So it is essential to investigate the effects of fullerene bisadduct regioisomers on photovoltaic performance.

Here, we report the isolation and photovoltaic performance of the regioisomers of NCBA. The *trans*-2, *trans*-3, *trans*-4, and *e* isomers of NCBA were isolated and used as acceptors for P3HT based PSCs, and the corresponding PSCs fabricated by the four isomers showed PCEs of 5.8, 6.3, 5.6, and 5.5%, respectively, which are higher than that based on NCBA mixture (5.3%), suggesting the necessity to use the individual fullerene bisadduct isomer for high performance PSCs.

2. Results and Discussion

2.1. Isolation

NCBA was synthesized and purified as reported previously.[14] The as-obtained NCBA mixture was further subjected to HPLC with a COSMOSIL 5PBB column. As shown in **Figure 2**, four peaks were mainly observed corresponding to four NCBA isomers. Four isomers clearly indicated the molecular ion peak corresponding to NCBA in MALDI-TOF mass spectra. By comparing the UV-Vis absorption spectrometry with other known fullerene bisadduct analogues,[19] the structure of each NCBA isomer can be unambiguously assigned as *trans*-2, *trans*-3, *trans*-4 and *e* isomer. Because the elution time of NCBA isomers depends on their polarity, the less polar *trans*-2 isomer is eluted first and followed by *trans*-3, *trans*-4 and *e* isomers. The *cis*-1, *cis*-2 and *cis*-3 isomers, where both adducts are present on the same hemisphere of the fullerene cage, were found to be low yield due to the steric hindrance. As for *trans*-1 isomer, the adducts are on opposite sides of the fullerene cage, leading to low yield due to the energetic unfavorable reactivity on this site.[19] This results in the NCBA mixture being heavily dominated by the *trans*-2, *trans*-3, *trans*-4 and *e* isomers. The photovoltaic performance of the *cis*-1, *cis*-2, *cis*-3 and *trans*-1 isomers were not investigated for their low yield.

2.2. Absorption Spectra

Figure 3 shows the UV-Vis absorption spectra of the four NCBA isomers in toluene. It was observed that the characteristic absorption spectra of the NCBA isomers are consistent with those of the corresponding fullerene bisadduct isomers reported before,[19] due to the fact that UV-Vis absorption spectra of fullerene bisadduct isomers is generally dependent on the addition patterns and almost independent of the kind of substituents on addends.[20] Immediately, the *e* isomer of NCBA was observed to own relatively weak absorption from 650 nm to 750 nm comparing with other three isomers, so it might lead to low current density due to the less solar absorption.

2.3. Electrochemical Property

The electrochemical properties of the NCBA isomers were measured using cyclic voltammetry. The cyclic voltammograms of the NCBA isomers exhibit three quasi-reversible reduction waves in the negative potential range from 0 to −2.5 V versus Ag/Ag^+ (Figure S2, see the Supporting Information). The LUMO energy levels of the NCBA isomers were estimated from their reduction onset potentials (E^{red}_{on}). As shown in **Table 1**, the LUMO energy levels of *trans*-2, *trans*-3, *trans*-4, and *e* isomers are estimated at −3.76, −3.70, −3.72 and −3.73 eV, respectively.

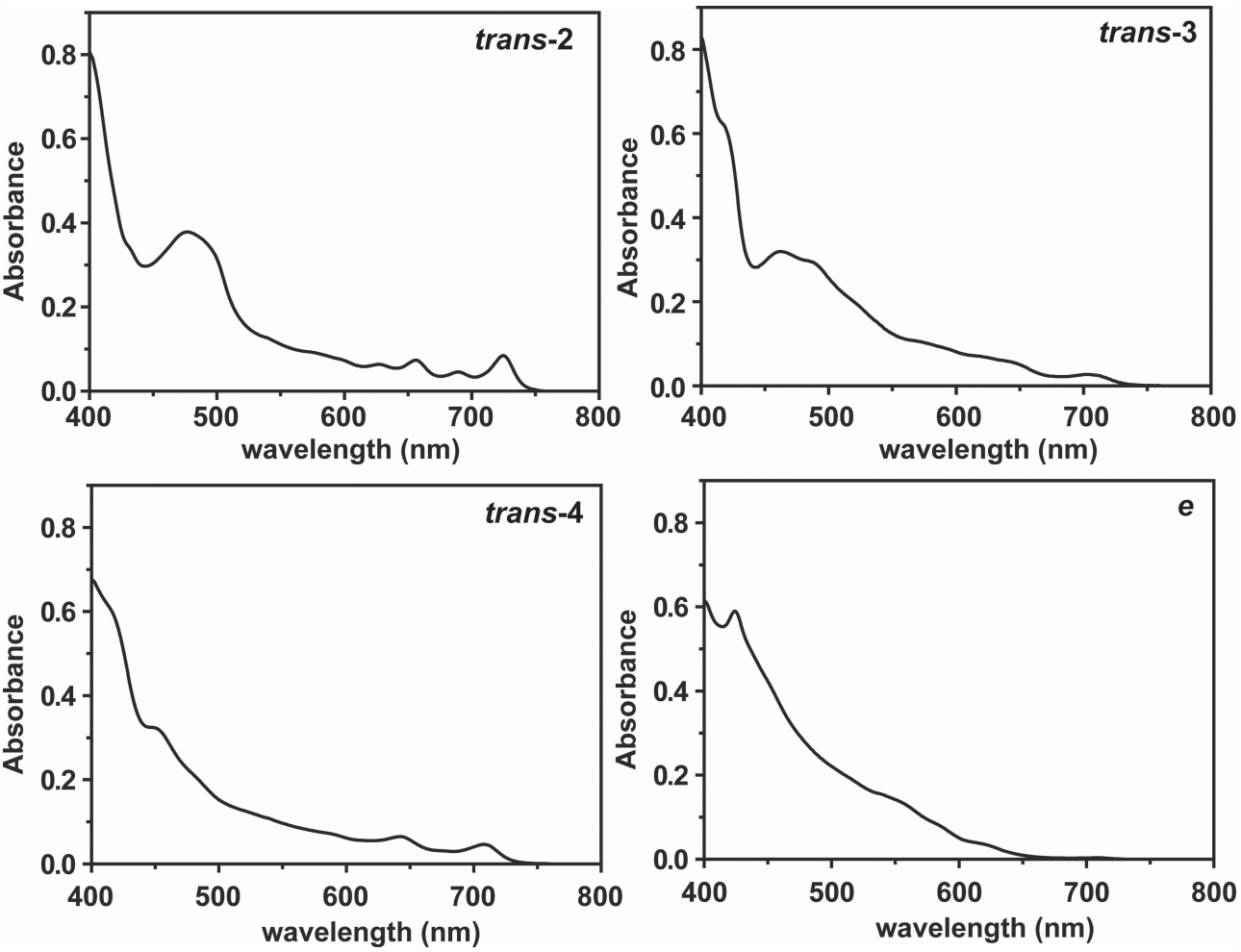

Figure 3. UV–vis absorption spectra of the NCBA isomers in toluene (10^{-4} mol/L).

Table 1. Electrochemical properties of the NCBA isomers.

isomers	E^{red}_{on} [V]	LUMO [eV]	calculated LUMO [eV]
trans-2	–0.95	–3.76	–2.95
trans-3	–1.01	–3.70	–2.85
trans-4	–0.99	–3.72	–2.85
e	–0.98	–3.73	–2.87
NCBA mixture	–0.95	–3.76	–

2.4. Theoretical Calculation

Density-functional theory (DFT) was also adopted to investigate the frontier orbitals of the individual NCBA isomers.[21] Based on the optimized geometries of the NCBA isomers at DFT B3LYP/6–31G(d) level, the LUMO levels were calculated as –2.95, –2.85, –2.85 and –2.87 eV for the *trans*-2, *trans*-3 *trans*-4, and *e* isomer, respectively, that are linearly consistent with the experimental results.

2.5. Photovoltaic Property

To evaluate the photovoltaic performance of the different NCBA isomers, PSCs based on the ITO/PEDOT:PSS/P3HT:acc-eptor/Ca/Al configuration were fabricated and characterized under the same conditions (Table S2, see the Supporting Information). The *J*–*V* curves of the PSCs based on P3HT:NCBA isomers (1:1, w/w) are shown in **Figure 4**, and the device performances are summarized in **Table 2**.

In Table 2, it can be seen that the device based on P3HT:*trans*-3 isomer has the V_{oc}, J_{sc}, and FF factor as high as 0.88 V, 10.21 mA/cm^2, and 0.71, respectively, affording the highest PCE of 6.3%, which is obviously superior to the NCBA mixture based PSC, and the performance improvements may be ascribed to following beneficial points on the *trans*-3 isomer of NCBA as acceptor. First, the *trans*-3 isomer has higher LUMO energy level than the NCBA mixture, resulting in higher V_{oc} of the PSC device. Second, the individual *trans*-3 isomer is favorable to reach regular molecular packing in the active layer, which usually lead to higher electron mobility and higher fill factor (FF) of the PSC device.

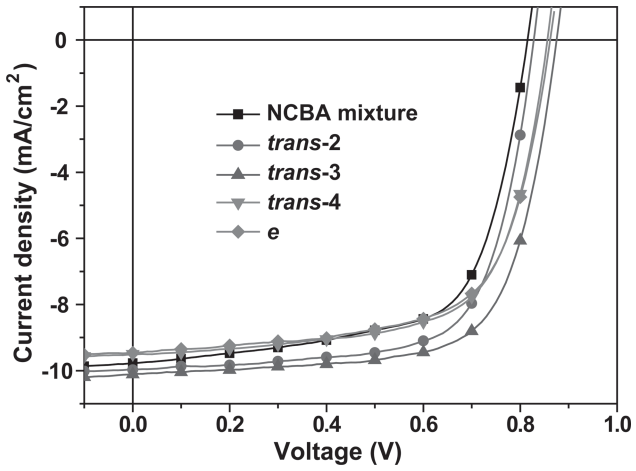

Figure 4. Current density-voltage curves of the PSCs based on P3HT:NCBA isomers (1:1, w/w).

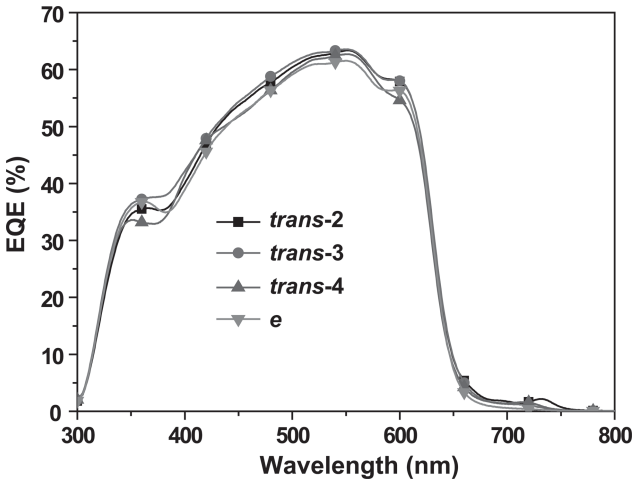

Figure 5. External quantum efficiency of the PSCs based on P3HT:NCBA isomers (1:1, w/w).

Table 2. Photovoltaic characteristics of the PSCs based on P3HT:NCBA isomers (1:1, w/w) under the illumination of AM1.5G, 100 mW/cm^2.

isomers	V_{oc} [V]	J_{sc} [mA/cm^2]	FF	PCE [%]
trans-2	0.83	10.04	0.69	5.8
trans-3	0.88	10.21	0.71	6.3
trans-4	0.86	9.67	0.67	5.6
e	0.86	9.51	0.67	5.5
NCBA mixture	0.82	9.88	0.67	5.3

Moreover, the NCBA isomers showed varying photovoltaic properties. It can be observed in Table 2 that the *trans*-2 isomer demonstrated slightly lower PCE of 5.8%. The decrease in the PCE of the P3HT:*trans*-2 isomer PSC compared to the *trans*-3 isomer based device was mainly due to a decrease in V_{oc}, which is caused by the lower LUMO energy level of the *trans*-2 isomer than the *trans*-3 isomer. Although the P3HT:*trans*-4 and P3HT:*e* isomer PSCs showed high V_{oc} of 0.86 V resulting from the elevated LUMO energy levels, their PCEs were measured only 5.6% and 5.5% perhaps due to film morphology, electron mobility and their weak absorption.

The external quantum efficiencies (EQE) of PSCs based on the NCBA isomers are shown in **Figure 5**. High EQE values over 60% in the wavelength range of 500–600 nm were observed in the devices, suggesting a high efficient photon-electron conversion process for the PSCs.

2.6. Morphology

The morphology of the P3HT:NCBA isomers blend films was examined by atomic force microscopy (AFM). The height images and phase images are shown in **Figure 6** (1 μm × 1 μm). There is no obvious difference in the morphology of the P3HT:NCBA isomers blend films. The surface RMS (root-mean-square) roughness of the films fabricated by P3HT:*trans*-2, P3HT:*trans*-3, P3HT:*trans*-4 and P3HT:*e* isomers are 5.1, 5.4, 5.2, and 4.6 nm, respectively. The relatively rough surface of the P3HT:NCBA isomers film is a signature of the P3HT self-organization after solvent annealing treatment, which would enhance ordered structural formation in the thin film. The phase image clearly shows the appearance of phase-separated domains with size of tens of nanometer, indicating the formation of a preferred film morphology in the blending layer that provided not only sufficient donor:acceptor interfaces for exciton dissociation but also effective pathways for charge transport.

2.7. Electron Mobility

The electron mobility of the NCBA isomers was measured by space charge limited current (SCLC) method (**Figure 7**). The *trans*-2 and *trans*-3 separately showed electron mobility of

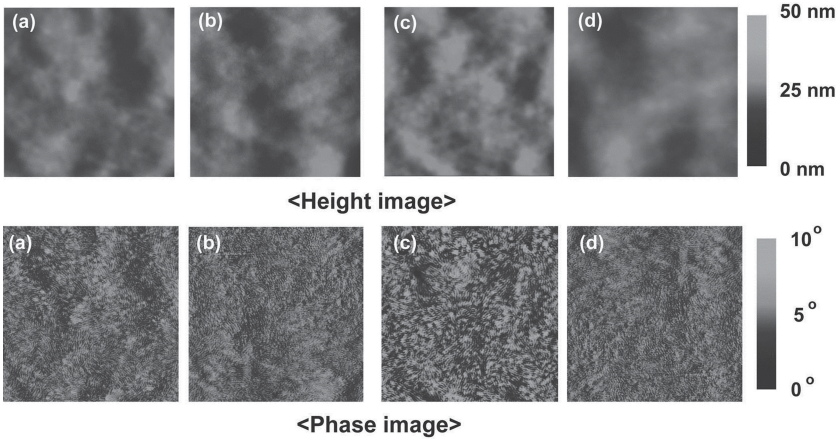

Figure 6. AFM height images (top line) and phase images (bottom line) of the blend films of P3HT with the NCBA isomers.

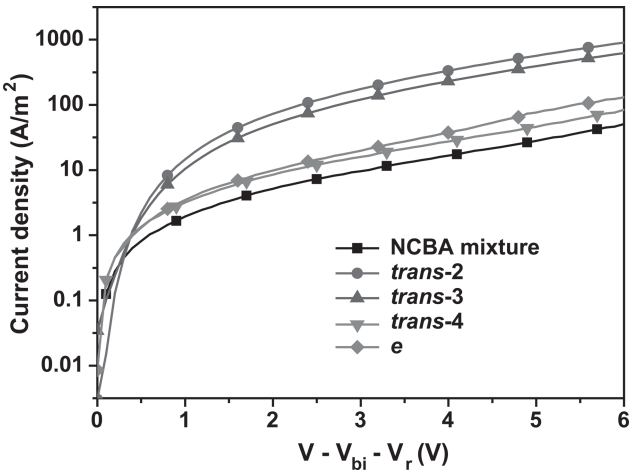

Figure 7. *J–V* curves for the electron-only devices based on P3HT:NCBA isomers blends under the same condition.

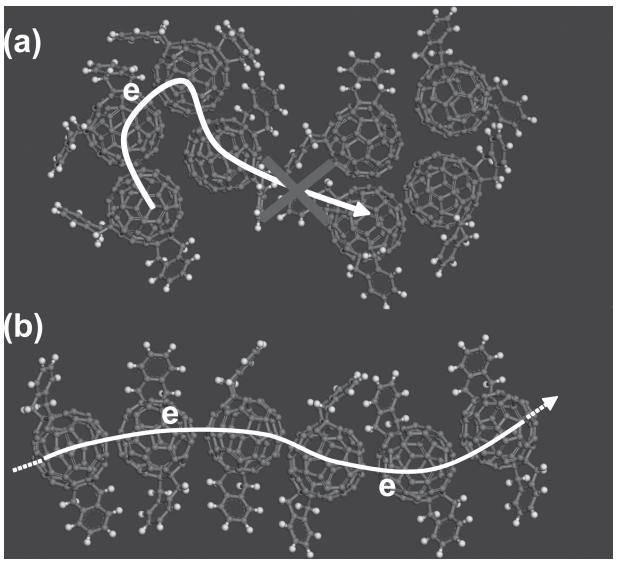

Figure 8. Illustrations of the molecular packing of a) the *e* isomer and b) the *trans*-2 isomer.

4.8×10^{-4} and 2.6×10^{-4} cm^2 V^{-1} s^{-1}, which are higher than the NCBA mixture (8.4×10^{-5} cm^2 V^{-1} s^{-1}). Undoubtedly, the relatively high charge carrier mobility of these NCBA isomers would bring the high photocurrents and fill factors in the PSC devices. Lower electron mobility of the *trans*-4 and *e* isomers was observed (9.6×10^{-5} and 9.4×10^{-5} cm^2 V^{-1} s^{-1}, respectively), corresponding to low J_{sc}, and FF.

2.8. Molecular Packing

We propose that the electron mobility is actually dictated by the ability of the fullerene cage to pack effectively.[22,23] The different fullerene cage packing of NCBA isomers may affect the ability of the fullerene channels to conduct electrons. The *trans*-4 and *e* isomers, when the two addends are attached nearly, are favorable to form small clusters in which the fullerene cages are π–π electronically coupled, and the insulating addends are positioned on the outside of the cluster (**Figure 8**a) restricting the electron mobility. Electron transport through the fullerene channels may be partially blocked by the outside insulating addends. In contrast, the *trans*-2 and *trans*-3 isomers are able to form extended structures where the π–π electronic coupling between the fullerene cages is undisturbed in the direction (Figure 8b). Fullerene cages can couple effectively to form channels for electron transport, leading to improved electron mobility.

3. Conclusions

Four isomers of NCBA, i.e., *trans*-2, *trans*-3, *trans*-4, and *e* isomers, were isolated and used as acceptors for P3HT based PSCs. The four NCBA isomers exhibit different absorption spectra, electrochemical property and electron mobility, leading to varying PCE values ranging from 5.5 to 6.3%. The P3HT:*trans*-3 isomer PSC afforded the highest PCE of 6.3%, which is obviously superior to the NCBA mixture based PSC (5.3%), and the performance improvements should be ascribed to higher LUMO energy level and higher electron mobility of the *trans*-3 isomer, suggesting the necessity to use the individual fullerene bisadduct isomer for high performance PSCs. Moreover, we found that the electron mobility of isomers is actually dictated by the ability of the fullerene cage to pack effectively. These findings indicate that the two substituent positions of the fullerene bisadduct does have a pronounced effect on absorption spectra, electrochemical property, electron mobility, and, therefore, overall photovoltaic performance. To further improve the photovoltaic performance of the fullerene bisadduct acceptors, it is important to isolate individual isomers post-synthesis or develop synthetic routes which preference particular isomers.

4. Experimental Section

Materials and Methods: P3HT (4002-E) was purchased from Rieke Metals Inc. Absorption spectra were taken on a Hitachi U-3010 UV-vis spectrophotometer. The electrochemical cyclic voltammetry was conducted on a Zahner IM6e Electrochemical Workstation. A Pt disk was taken as the working electrode, Pt wire as the counter electrode, and Ag/Ag^+ electrode (0.01 M $AgNO_3$, 0.09 M NBu_4PF_6 in acetonitrile) as the reference electrode. A mixed solution of *o*-dichlorobenzene:aceton itrile (v:v = 5:1) with 0.1 M tetrabutylammonium hexafluorophosphate (NBu_4PF_6) was used as electrolyte, and the scan rate was fixed at 100 mV s^{-1}. High performance liquid chromatography (HPLC) analysis was performed on LC908-C60 (Jai CO., LTD.). The AFM images under tapping mode were taken on a Veeco NanoScope IIIa SPM (DI, USA).

Computational Details: All isomers were optimized at the B3LYP/6–31G(d) level of density functional theory. All calculations were carried out with the Gaussian 03 program.

Fabrication and Characterization of PSCs: The PSCs were fabricated in the configuration of the traditional sandwich structure ITO/PEDOT:PSS/BHJ/Ca/Al. The ITO glass was cleaned by sequential ultrasonic treatment in detergent, deionized water, acetone, and isopropanol, and then treated in an ultraviolet-ozone chamber (Ultraviolet Ozone Cleaner, Jelight Company, USA) for 20 min. Then PEDOT:PSS (poly (3,4-ethylene dioxythiophene):poly(styrene sulfonate)) (Baytron PVPAI

4083, Germany) was filtered through a 0.45 μm filter and spin coated at 2500 rpm for 35 s on the ITO electrode. Subsequently, the PEDOT:PSS film was baked at 150 °C for 20 min in the air. The blend solution of P3HT and different fullerene derivative acceptors in dichlorobenzene (DCB) (total concentration is 34 mg mL^{-1}, weight ratio of P3HT:Acceptor of 1:1) was spin-coated on top of the PEDOT:PSS layer. The blend films were then put into glass petridishes while still wet to undergo solvent annealing process. The thickness of the photoactive layer was estimated by Surface Profiler in the range of 180–240 nm. The device was annealed at 150 °C for 10 min. A bilayer cathode consisted of Ca (20 nm) capped with Al (100 nm) was thermal-evaporated under a shadow mask in a base pressure of ca. 10^{-4} Pa. The device active area of the PSCs is ca. 4 mm^2. The *J–V* measurement of the devices was conducted on a computer-controlled Keithley 236 Source Measure Unit. Device characterization was done in golvebox under simulated AM1.5G irradiation (100 mW cm^{-2}) using a xenon-lamp-based solar simulator (from Newport Co., LTD.). The EQE measurements of the PSCs were performed by Stanford Research Systems model SR830 DSP lock-in amplifier coupled with WDG3 monochromator and 500 W xenon lamp. The light intensity at each wavelength was calibrated with a standard single-crystal Si photovoltaic cell.

Space Charge Limited Current (SCLC) Measurements: The electron mobility was measured by the space charge limited current (SCLC) method by an electron-only device with a tructure of ITO/TIPD/Active layer/Ca/Al.[24] The measurement of electron mobilities was conducted in the dark on a computer-controlled Keithley 236 Source Measure Unit. The SCLC electron mobility was estimated the Mott-Gurney square law $J = 9(\varepsilon_0\varepsilon_r\mu)/8 \times (V^2/d^3)$, where j is current density, ε_0 is the permittivity of vacuum, ε_r is dielectric constant of the fullerene derivatives, μ is electron mobility, $V = V_{appl} - V_{bi} - V_r$, V_{appl} is the applied potential, V_{bi} is the built-in potential resulting from workfunction difference between two electrodes, V_r is the voltage drop due to the resistance, and d is film thickness.

Supporting Information

Supporting Information is available from the Wiley Online Library or from the author.

Acknowledgements

This work was supported by the National Basic Research Program (2012CB932900), and the NSFC (Nos. 91027018, 11179006, 21273006, 21121063, 51002102 and 51072200).

Received: April 25, 2013
Revised: June 26, 2013
Published online: July 19, 2013

[1] a) S. Gunes, H. Neugebauer, N. S. Sariciftci, *Chem. Rev.* **2007**, *107*, 1324; b) B. C. Thompson, J. M. J. Frechet, *Angew. Chem. Int. Ed.* **2008**, *47*, 58; c) L. M. Chen, Z. R. Hong, G. Li, Y. Yang, *Adv. Mater.* **2009**, *21*, 1434; d) G. Dennler, M. C. Scharber, C. J. Brabec, *Adv. Mater.* **2009**, *21*, 1323.

[2] G. Yu, J. Gao, J. C. Hummelen, F. Wudl, A. J. Heeger, *Science* **1995**, *270*, 1789.

[3] Z. He, C. Zhong, S. Su, M. Xu, H. Wu, Y. Cao, *Nat. Photon.* **2012**, *6*, 591.

[4] a) L. Dou, J. You, J. Yang, C. C. Chen, Y. He, S. Murase, T. Moriarty, K. Emery, G. Li, Y. Yang, *Nat. Photon.* **2012**, *6*, 180; b) L. Dou, W.-H. Chang, J. Gao, C.-C. Chen, J. You, Y. Yang, *Adv. Mater.* **2013**, *25*, 825; c) J. You, L. Dou, K. Yoshimura, T. Kato, K. Ohya, T. Moriarty, K. Emery, C.-C. Chen, J. Gao, G. Li, Y. Yang, *Nat. Commun.* **2013**, *4*, 1446.

[5] a) J. Chen, Y. Cao, *Acc. Chem. Res.* **2009**, *42*, 1709; b) Y.-J. Cheng, S.-H. Yang, C.-S. Hsu, *Chem. Rev.* **2009**, *109*, 5868; c) Y. Li, *Acc. Chem. Res.* **2012**, *45*, 723.

[6] a) Y. He, Y. Li, *Phys. Chem. Chem. Phys.* **2011**, *13*, 1970; b) C. Z. Li, H. L. Yip, A. K. Y. Jen, *J. Mater. Chem.* **2012**, *22*, 4161.

[7] C. J. Brabec, A. Cravino, D. Meissner, N. S. Sariciftci, T. Fromherz, M. T. Rispens, L. Sanchez, J. C. Hummelen, *Adv. Funct. Mater.* **2001**, *11*, 374.

[8] a) R. B. Ross, C. M. Cardona, D. M. Guldi, S. G. Sankaranarayanan, M. O. Reese, N. Kopidakis, J. Peet, B. Walker, G. C. Bazan, E. Van Keuren, B. C. Holloway, M. Drees, *Nat. Mater.* **2009**, *8*, 208; b) R. B. Ross, C. M. Cardona, F. B. Swain, D. M. Guldi, S. G. Sankaranarayanan, E. Van Keuren, B. C. Holloway, M. Drees, *Adv. Funct. Mater.* **2009**, *19*, 2332; c) F. B. Kooistra, J. Knol, F. Kastenberg, L. M. Popescu, W. J. H. Verhees, J. M. Kroon, J. C. Hummelen, *Org. Lett.* **2007**, *9*, 551.

[9] a) G. Zhao, Y. He, Z. Xu, J. Hou, M. Zhang, J. Min, H.-Y. Chen, M. Ye, Z. Hong, Y. Yang, Y. Li, *Adv. Funct. Mater.* **2010**, *20*, 1480; b) K.-H. Kim, H. Kang, S. Y. Nam, J. Jung, P. S. Kim, C.-H. Cho, C. Lee, S. C. Yoon, B. J. Kim, *Chem. Mater.* **2011**, *23*, 5090; c) Y. He, B. Peng, G. Zhao, Y. Zou, Y. Li, *J. Phys. Chem. C.* **2011**, *115*, 4340; d) C.-Z. Li, S.-C. Chien, H.-L. Yip, C.-C. Chueh, F.-C. Chen, Y. Matsuo, E. Nakamura, A. K. Y. Jen, *Chem. Commun.* **2011**, *47*, 10082; e) E. Voroshazi, K. Vasseur, T. Aernouts, P. Heremans, A. Baumann, C. Deibel, X. Xue, A. J. Herring, A. J. Athans, T. A. Lada, H. Richter, B. P. Rand, *J. Mater. Chem.* **2011**, *21*, 17345; f) X. Y. Meng, W. Q. Zhang, Z. A. Tan, Y. F. Li, Y. H. Ma, T. S. Wang, L. Jiang, C. Y. Shu, C. R. Wang, *Adv. Funct. Mater.* **2012**, *22*, 2187; g) X. Y. Meng, Q. Xu, W. Q. Zhang, Z. A. Tan, Y. F. Li, Z. X. Zhang, L. Jiang, C. Y. Shu, C. R. Wang, *ACS Appl. Mater. Interfaces* **2012**, *4*, 5966; h) G. Ye, S. Chen, Z. Xiao, Q. Zuo, Q. Wei, L. Ding, *J. Mater. Chem.* **2012**, *22*, 22374.

[10] M. Lenes, G. Wetzelaer, F. B. Kooistra, S. C. Veenstra, J. C. Hummelen, P. W. M. Blom, *Adv. Mater.* **2008**, *20*, 2116.

[11] Y. J. He, H. Y. Chen, J. H. Hou, Y. F. Li, *J. Am. Chem. Soc.* **2010**, *132*, 1377.

[12] Y.-J. Cheng, M.-H. Liao, C.-Y. Chang, W.-S. Kao, C.-E. Wu, C.-S. Hsu, *Chem. Mater.* **2011**, *23*, 4056.

[13] C. Zhang, S. Chen, Z. Xiao, Q. Zuo, L. Ding, *Org. Lett.* **2012**, *14*, 1508.

[14] X. Y. Meng, W. Q. Zhang, Z. A. Tan, C. Du, C. H. Li, Z. S. Bo, Y. F. Li, X. L. Yang, M. M. Zhen, F. Jiang, J. P. Zheng, T. S. Wang, L. Jiang, C. Y. Shu, C. R. Wang, *Chem. Commun.* **2012**, *48*, 425.

[15] A. Hirsch, I. Lamparth, H. R. Karfunkel, *Angew. Chem. Int. Ed.* **1994**, *33*, 437.

[16] R. K. M. Bouwer, G. J. A. H. Wetzelaer, P. W. M. Blom, J. C. Hummelen, *J. Mater. Chem.* **2012**, *22*, 15412.

[17] S. Kitaura, K. Kurotobi, M. Sato, Y. Takano, T. Umeyama, H. Imahori, *Chem. Commun.* **2012**, *48*, 8550.

[18] J. M. Frost, M. A. Faist, J. Nelson, *Adv. Mater.* **2010**, *22*, 4881.

[19] a) Y. Nakamura, K. O-kawa, M. Matsumoto, J. Nishimura, *Tetrahedron* **2000**, *56*, 5429; b) Y. Nakamura, N. Takano, T. Nishimura, E. Yashima, M. Sato, T. Kudo, J. Nishimura, *Org. Lett.* **2001**, *3*, 1193.

[20] K. Kordatos, S. Bosi, T. Da Ros, A. Zambon, V. Lucchini, M. Prato, *J. Org. Chem.* **2001**, *66*, 2802.

[21] Z. Zhang, P. Han, X. Liu, J. Zhao, H. Jia, F. Zeng, B. Xu, *J. Phys. Chem. C* **2008**, *112*, 19158.

[22] N. C. Miller, S. Sweetnam, E. T. Hoke, R. Gysel, C. E. Miller, J. A. Bartelt, X. Xie, M. F. Toney, M. D. McGehee, *Nano Lett.* **2012**, *12*, 1566.

[23] A. M. Nardes, A. J. Ferguson, J. B. Whitaker, B. W. Larson, R. E. Larsen, K. Maturová, P. A. Graf, O. V. Boltalina, S. H. Strauss, N. Kopidakis, *Adv. Funct. Mater.* **2012**, *22*, 4115.

[24] Z. A. Tan, W. Zhang, Z. Zhang, D. Qian, Y. Huang, J. Hou, Y. Li, *Adv. Mater.* **2012**, *24*, 1476.